Melt Rheological and Compatibility Properties of Recycled Poly(ethylene terephthalate)/ Poly(acrylonitrile-butadiene-styrene) Blends

Hai Wang, Qingrong Qian, Xia Jiang, Xinping Liu, Liren Xiao, Baoquan Huang, Qinghua Chen

College of Chemistry and Materials Science, Fujian Normal University, Fuzhou 350007, China

Received 4 January 2012; accepted 8 February 2012
DOI 10.1002/app.36984
Published online in Wiley Online Library (wileyonlinelibrary.com).

ABSTRACT: In this study, a series of maleic anhydride (MA)-grafted poly(acrylonitrile-butadiene-styrene) (ABS-*g*-MAH) were prepared via a melt banbury process on a RM-200B torque rheometer and used as a compatibilizer for recycled poly(ethylene terephthalate)/poly(acrylonitrile-butadiene-styrene) (R-PET/ABS) blends. The melt rheological and compatibility properties of R-PET/ABS blends were investigated. It had been found that 5 wt % of MA was an optimum concentration for the preparation of ABS-*g*-MAH. About 1 wt % of ABS-*g*-MAH prepared at the MA optimum conditions shows good compatibility for the basic blend of R-PET/ABS 85/15 w/w. Rheological and SEM characterizations confirmed that the phase reversal of blends occurred at R-PET/ABS ratio of 75/25 w/w. DMA results indicated that R-PET was partially miscible with ABS, and ABS-*g*-MAH was an efficient compatibilizer for R-PET/ABS blends. © 2012 Wiley Periodicals, Inc. J Appl Polym Sci 000: 000–000, 2012

Key words: R-PET/ABS blends; rheological property; phase reversal; morphology property; compatibilizer

INTRODUCTION

Plastic waste recycling conserves both material and energy and provides a comparatively simple way to make a substantial reduction in the overall volume of municipal solid waste. PET bottles constitute a significant fraction of the plastic wastes and represent an important recycling opportunity.[1] High consumption of PET bottles in packaging industry may inevitably lead to large amounts of plastic wastes, which may cause a serious environmental problem due to their chemically stability. During last decades, numerous methods have been developed to recycle PET wastes, including blending the recycled PET (R-PET) with virgin PET, polyolefins, and polyesters, modifying it by chain extenders, incineration, and chemical recycling. Among these methods, blending R-PET with other polymers is very attractive due to the ease of fabrication, economy, and superior mechanical properties of the blends.[2,3] The blending of two dissimilar polymers offers the potential of providing a material with the advantages of each and at a fraction of the research costs normally associated with the synthesis of new polymer systems. In general, the polymers are selected on the basis of the particular properties that they may offer in the blended state such as toughness, chemical resistance, or heat stability. However, the rule of mixtures (which predicts that blend properties will be the average of their ingredients) generally does not hold in polymer blends, because the blend components are usually not totally miscible and form a two-phase structure. Conventional wisdom in blending immiscible polymers states that optimum blend properties are obtained by the use of a compatibilizer, which has two or more segments, which are miscible with one of the two blend phases but not with both. These compatibilizers are believed to function by reducing the interfacial energy and stabilizing the domain structure. In some circumstances, this may also lead to the development of a cocontinuous structure in which each phase interpenetrates the other, and such a morphology may provide valuable properties. The compatibilizer may also improve adhesion between the domains and aid stress transfer between them.[4] Li and Lu[5] had demonstrated the melt rheological properties of HDPE/PET blends compatibilized by an ethylene-butyl-acrylate-glycidyl methacrylate

Correspondence to: Q. Qian (qrqian@fjnu.edu.cn) or Q. Chen (cqhuar@pub5.fz.fj.cn).

Contract grant sponsor: Fujian Provincial Government (Major Special Science and Technology Project); contract grant number: 2007 HZ0001-1.

Contract grant sponsor: Fujian Engineering Research Center of Environment-Friendly Polymer Material; contract grant number: 2009H2004.

terpolymer (EBAGMA) by means of a HAAKE torque rheometer and a capillary rheometer. The results showed that the melts of blends behaved in a pseudoplastic manner. The addition of EBAGMA enhanced the interfacial adhesion between HDPE and PET and improved the phase dispersion due to reactive compatibilization. Calderas[6] had studied the rheological properties of PET/SBR and PET with maleic anhydride (MA) grafted styrene butadiene rubber (SBRg) blends with a special capillary device. The results showed that grafted MA chains at the rubber-thermoplastic interface affect the rheological properties of the blends. Silva and Bretas[7] had studied the blends of a bottle grade polyethylene terephthalate (PET) copolymer with a liquid crystalline polymer by injection molding. The viscosity measurements gave an indication that the interface was strong, probably due to transesterification reactions that occurred during the process.

This work was a system of MA-grafted poly(acrylonitrile-butadiene-styrene) (ABS-*g*-MAH) copolymer being prepared and engineering blends being formed from the tough nonpolar thermoplastic styrenic polymer, ABS, and an oil-resistant polar semicrystalline polyester, recycled poly(ethy1ene terephthalate) (R-PET)[8] using the prepared ABS-*g*-MAH as a compatibilizer via torque rheology. The primary aim in blending the tough amorphous thermoplastic ABS with R-PET is to combine the high impact strength of ABS with the solvent resistance, good mechanical properties, and processability of R-PET. However, PET and ABS are immiscible and require compatibilization.[9] Cook et al.[10,11] have studied that the uncompatibilized PET/ABS blends were immiscible and consisted of four phases: styrene-aerylonitrile copolymer, grafted polybutadiene, amorphous PET, and small amounts of crystalline PET. Meanwhile, uncompatibilized blends quenched from the melt showed good tensile properties, but these deteriorated during storage at room temperature because of debonding of ABS particles. Grafting of ABS-*g*-MAH particles onto the PET matrix led to compatibilization, resulting in stable properties.[12] The R-PET/ABS blends with ABS-*g*-MAH as compatibilizer might be commercially significant, and it might partially replace the more expensive PC/ABS blends being used in automotive applications.

EXPERIMENTAL

Materials

R-PET flakes used in this study were friendly provided by Long-Cheng Company, Fuzhou, China. The as-received R-PET flakes were dried in a DHG Series heating and drying oven at 120°C for 12 h to keep very low moisture content. The polymer had an intrinsic viscosity of 0.59 dL/g, measured in a 1/1 (wt) mixture of phenol and tetrachloroethane at 25°C. ABS (PKA-757S) purchased from Qi Mei Enterprise Co., (Taiwan, China) was dried at 80°C for 12 h in a vacuum oven before melt processing. MA and dicumyl peroxide (DCP; obtained from Sinopharm Chemical Reagent Co.) were used as a grafting monomer and radical initiator, respectively. All chemicals were used without any purification.

Preparation

The preparation of MA-grafted poly(acrylonitrile-butadiene-styrene) (ABS-*g*-MAH) in the molten state was performed in a RM-200B torque rheometer with a 50-mL mixing head (operated at 205°C and 40 rpm). The mixing time was about 6 min for each sample to record the change of torque as a function of residence time with the content of MA varied from 1 to 7 wt % and DCP fixed 0.5 wt %. The untreated ABS pellets are referred to UT, and the ABS pellets treated with 1.0, 3.0, 5.0, and 7.0 wt % of MA were denoted by T1.0, T3.0, T5.0, and T7.0, respectively. The ABS-*g*-MAH prepared with the content of MA 5 wt % was used as a compatibilizer for R-PET/ABS blends.

Previous studies were performed on a torque rheometer to optimize the mixing time, temperature, and rotation speed in the melt process. It is clear that the processing temperature of recycled PET used in this study is lower than that of virgin PET. The R-PET/ABS blends with different compositions and R-PET/ABS(85/15) w/w with different content of ABS-*g*-MAH compatilizer were prepared in a torque rheometer (RM-200B, China) with a 50-mL mixing head (operated at 260°C and 40 rpm). In a typical experiment, R-PET flakes and ABS pellets were dried overnight to ensure moisture content less than 0.1 wt %. Approximately 60 g of premixed mixture was added in the intensive mixer heated at a preset chamber temperature of 260°C. R-PET/ABS ratio was changed from 95/5 to 55/45 w/w, and the content of ABS-*g*-MAH compatilizer was varied from 1 to 5 wt %.

Measurements

The purified samples were pressed to obtain films whose thicknesses were about 40–60 μm. The FTIR spectra of ABS, MA, and ABS-*g*-MAH were obtained using a Thermo Nicolet 5700 FTIR spectrometer. The grafted degree (GD) of MAH was determined by a back-titration procedure. The purified sample (1.0 g) was dissolved in 100 mL acetone, and then 10 mL of an ethanol solution of NaOH (0.1 mol/L) was added. The mixed solution was refluxed for 30 min with stirring and then back-titrated with 0.1 mol/L

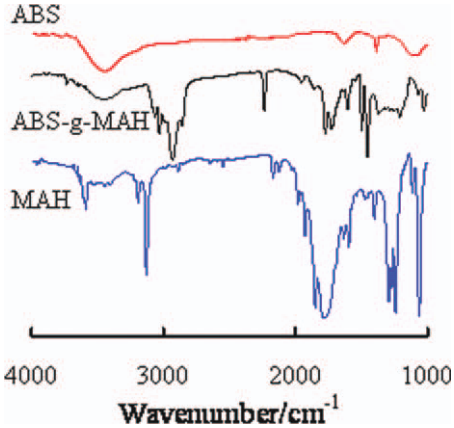

Figure 1 The FTIR spectra of maleic anhydride grafted poly(acrylonitrile-butadiene-styrene). [Color figure can be viewed in the online issue, which is available at wileyonlinelibrary.com.]

HCl using methyl red as an indicator. GD was defined as the amount of grafted MAH as a percentage of ABS:

$$\mathrm{GD}(\%) = \frac{(V_o - V_1) \times 10^{-3} \times C \times M}{2W} \times 100$$

where V_0 is the amount of HCl consumed with pure ABS as a reference (mL), V_1 is the amount of HCl consumed by the grafted sample (mL), C is the molar concentration of HCl (mol/L), M is the molecular weight of MAH, and W is the weight of the sample (g).

Storage modulus G' and loss modulus G'' values as a function of frequency for all samples were collected on a Rheometer AR-2000 with a parallel plate mode. The AR-2000 system was programmed to perform frequency sweeps within the range of 0.1–100 rad/s at 260°C for R-PET/ABS blends and at 210°C for ABS-*g*-MAH samples. Specimens were discs with 25 mm radius and 3 mm thickness. The discs were prepared by compression-molding immediately after the melting reaction and stored at room temperature for 24 h to keep the stability of structures before the measurement.

The dynamic mechanical analysis (DMA) measurements were conducted on a Q800 TA Instrument using a sample in size of 35 × 13 × 3 mm. The tan δ was obtained at the frequency of 5 Hz with the amplitude of 20.00. The heating rate was 2.0°C/min.

SEM images of the etched fracture surface of various blends were recorded to investigate the changes in phase morphology. The samples were fractured in liquid nitrogen perpendicular to the direction of flow. The fracture surface of the blends was etched with butanone at room temperature for 12 h to remove the ABS phase. After room-temperature drying of the surface, the surface of specimens was cut and then gold-coated for SEM (JEOL JSM-7500F) examination, which was carried out at an accelerated voltage of 5 kV.

Flexural properties were tested by CMT-4004 Mechanical Properties Testing Machine, according to Chinese Standard GB/T9341-2000 at 23°C. Charpy impact strength was performed by ZBC1400-2 Impact Tester, according to Chinese Standard GB/T1043-1993 at 23°C. Both testing machines were manufactured by Sans Mechanical Properties Testing Machine (Shengzhen, China).

RESULTS AND DISCUSSION

Characterization of ABS-*g*-MAH

FTIR analysis

The grafting product was dissolved in 1,2-dichloroethane, and the unreacted MAH in the solution was extracted by adding ethanol. The purified ABS-*g*-MAH polymer was dried to constant weight in a vacuum oven at 80°C before the FTIR characterization. Figure 1 shows the FTIR spectra of raw ABS, MAH, and ABS-*g*-MAH (T5.0) polymer. Compared to the FTIR spectra of raw ABS and MA, the appearance of a new absorbance bands at 1778 and 1730 cm^{-1} (C=O stretching from anhydride) in ABS-*g*-MAH indicates that the MA is successfully introduced onto ABS by grafting. Ma et al.[13] have reported that the grafting of MAH takes place in the butadiene phase of ABS.

Rheology analysis

The plots of G' versus G'', so-called Cole–Cole plots, for ABS-*g*-MAH copolymers with different MA concentrations at 210°C are shown in Figure 2. It is a well-known fact that the homogeneous and isotropic

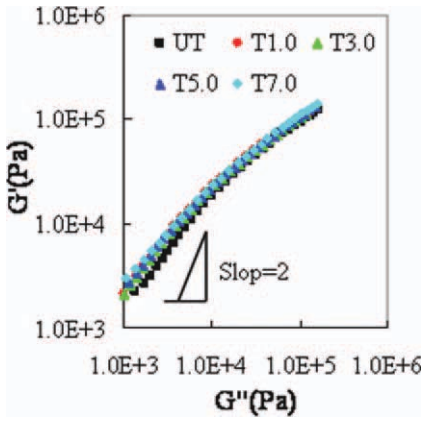

Figure 2 G' versus G'' plots for ABS-*g*-MAH polymers with different maleic anhydride contents at 210°C. [Color figure can be viewed in the online issue, which is available at wileyonlinelibrary.com.]

TABLE I
Effect of the Monomer Concentration on the Grafted Degree

Monomer concentration (phr)	Grafted degree (%)
0	0.00
1	0.95
3	2.82
5	4.69
7	4.71

polymer melts/solutions give a slope of plot as 2, and the slop deviates from 2 with the heterogeneity increase.[13,14] The curve of T7.0 gives a higher slope value and deviations from the master curve corresponding to UT, T1.0, T3.0, and T5.0. The excess dose of MA acts as a plasticizer in the polymeric systems and, as a result, shifts the Cole–Cole plot to higher G'' at a constant value of G' and gives rise to a notable increase in the degree of heterogeneity.[14] Accordingly, in our experimental conditions, 5 wt % of MA is suggested to be an optimum concentration for the preparation of ABS-*g*-MAH polymer.

Back-titration analysis

Table I shows that the DG increases from 0.95 to 4.69% by increasing MA concentration from 1.0 to 5.0%, suggesting that the number of monomer molecules reaching the polymer backbone governed the extent of grafting. However, at a high-monomer concentration, the extra monomer acts as a trap for ABS radicals,[15] resulting in low-grafting reaction rate. This is the reason why the DG of ABS-*g*-MAH polymer with 5 wt % MA is approximate to that of with 7 wt % MA.

Characterization of R-PET/ABS blends

Melt rheology

In Figure 3, the evolution of the storage modulus (G') and loss modulus (G'') of the R-PET/ABS blends without any compatibilizer is presented together with that of the neat polymers at 260°C. In the whole frequency range investigated, G' and G'' values of pure ABS are found to be the highest among all samples. And they are observed to increase with increasing ABS proportion for R-PET/ABS blends. However, R-PET/ABS blends with low-ABS proportion (95/5 and 85/15 w/w) have lower G' and G'' values in whole frequency range, whereas those with high ABS content (75/25, 65/35, and 55/45 w/w) blends possess higher G' and G'' values in the low frequency range in comparison with R-PET. This phenomenon is known as an interfacial tension effect and has been extensively addressed in the literature in the case of polymer blends even from a theoretical point of view.[16] Indeed, in the case of dispersed droplets in a continuous matrix, this effect has been reported as the excess of elasticity or as the occurrence of long relaxation times. It is related to the deformability of the dispersed phase, which gives rise to a shape relaxation. This process is clearly connected to the behavior of the neat polymers, but the volume fraction of dispersed phase, the size, and, to a lower extent, the distribution of size and the interfacial tension has the most important effects. The phenomenon is also observed in other morphologies such as full or partial cocontinuous morphologies. Thus, more generally, the relevant parameter is the interfacial energy, product of the interfacial area with the interfacial tension. The study of Carrot et al.[17] has reported that the effect is rather small for cocontinuous morphologies, because, in this case, the interfacial area is generally smaller than for dispersed phases. In Figure 3, the phenomenon is particularly pronounced for blends 85/15 and 95/5 w/w, which show entire frequency scale relaxation and a typical R-PET matrix-ABS droplets morphology. Moreover, it is notable that the G' and G'' for blend 75/25 w/w increases dramatically, and this phenomenon suggests that phase inversion of the blend occurs between 75/25 and 65/35 in weight ratio.[18]

Figure 4 shows the evolution of the storage modulus G' and loss modulus G'' for R-PET/ABS blends 85/15 w/w with different ABS-*g*-MAH concentrations of 0.0, 1.0, 3.0, and 5.0 wt % (noted as G_1, G_2, G_3, and G_4, respectively). The presence of ABS-*g*-MAH polymer causes increase in G' and G'' values over the entire frequency range, especially in the low frequency, indicating an enhanced interaction between phases due to compatibilizer. However, the values of G' and G'' show a little decrease with increase in amount of ABS-*g*-MAH polymer from 1.0 to 3.0 wt % and almost no change from 3.0 to 5.0 wt %. This result suggests that the optimum concentration of ABS-*g*-MAH polymer used for compatibilizing R-PET/ABS blend 85/15 w/w is ~ 1.0 wt %.[10]

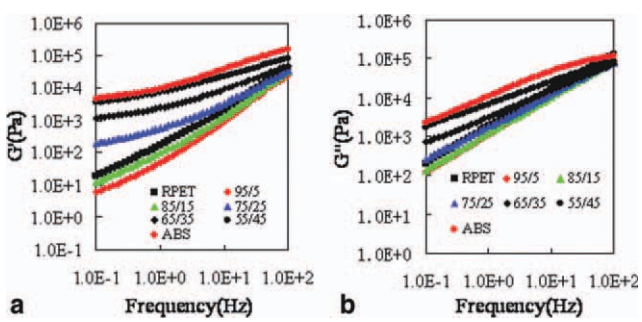

Figure 3 (a) Storage modulus and (b) loss modulus of ABS, R-PET, and various R-PET/ABS blends at 260°C. [Color figure can be viewed in the online issue, which is available at wileyonlinelibrary.com.]

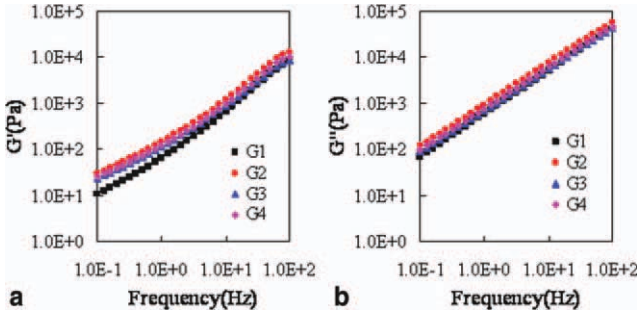

Figure 4 Changes in storage modulus (a) and loss modulus (b) as a function of frequency for R-PET/ABS blends with various concentrations of compatibilizer at 260°C. [Color figure can be viewed in the online issue, which is available at wileyonlinelibrary.com.]

Morphology

Morphology of R-PET/ABS blends was investigated by SEM. Because of the weak phase contrast between R-PET and ABS, the ABS phase of the blend fracture surface was removed by butanone etching to form cavity without affecting the R-PET phase. Figure 5 shows SEM images for butanone-etched fracture surface of R-PET/ABS blends with various R-PET/ABS ratios. As is illuminated in Figure 5(a,b), R-PET/ABS blends with 95/5 and 85/15 w/w ratios possess a typical two-phase structure. Small ABS particles disperse as an island phase in R-PET matrix. It is clear that most of butanone-etched cavities give sharp boundaries and smooth surface, suggesting that there is little or no adhesion between the R-PET and ABS phase due to their poor compatibility. However, the disperse phase ABS in R-PET/ABS blend with 75/25 w/w ratio clearly shows an elongated or clavate structure in R-PET matrix morphology [Fig. 5(c)]; meanwhile, there are interconnecting spherulites R-PET as disperse phase located in the ABS matrix, indicating the interesting double sea islands structure being formed and the occurrence of phase inversion. The novel double sea island structure formed is attributed to the disparity of viscosity between R-PET and ABS. It is interesting to note that the cocontinuous structure of the binary polymer blend is formed in the R-PET/ABS ratio range of 65/35 and 55/45 w/w attributed to the droplet–droplet coalescence, suggesting the complete of the phase inversion.[19,20] Accordingly, the R-PET/ABS blend ratios between 75/25 and 65/35 w/w have been considered as the critical point of phase inversion for the present blend systems.

Figure 6 shows the SEM images of ABS-*g*-MAH-compatibilized R-PET/ABS (85/15 w/w) blends. The R-PET/ABS (85/15 w/w) blends compatibilized by 1.0 and 3.0 wt % ABS-*g*-MAH show finer morphologies. The boundaries of the cavities are obscure and seemed to be more difficult to etch, indicating that the interfacial adhesion is markedly improved.[21,22] However, the boundaries of the cavities are transformed distinctly when the compatibilizer content is increased to 5 wt %. At a high-ABS-*g*-MAH concentration, the excess compatibilizer may form the third phase in the R-PET/ABS system without transferred to interphase and cannot play as an effective role of compatibility. Generally, the phase morphology of polymer blends is assumed to be

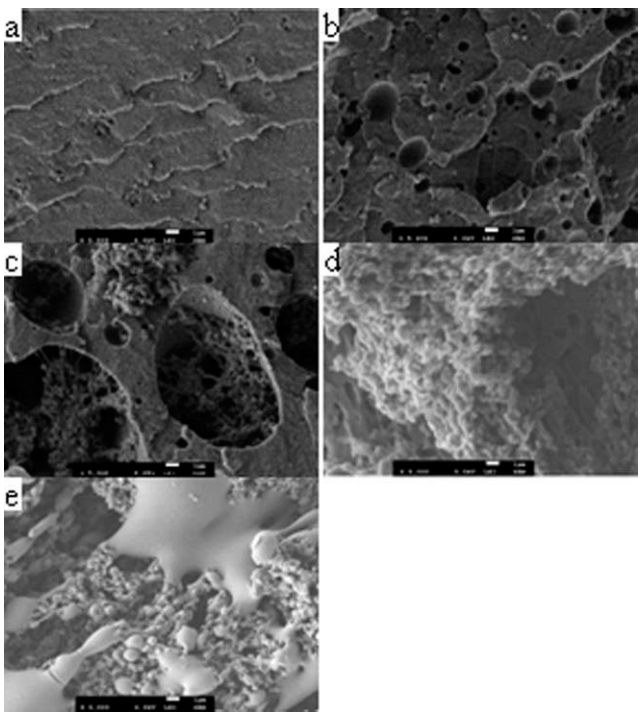

Figure 5 SEM images for the R-PET/ABS blends with various blending ratios (w/w): (a) 95/5, (b) 85/15, (c) 75/25, (d) 65/35, and (e) 55/45.

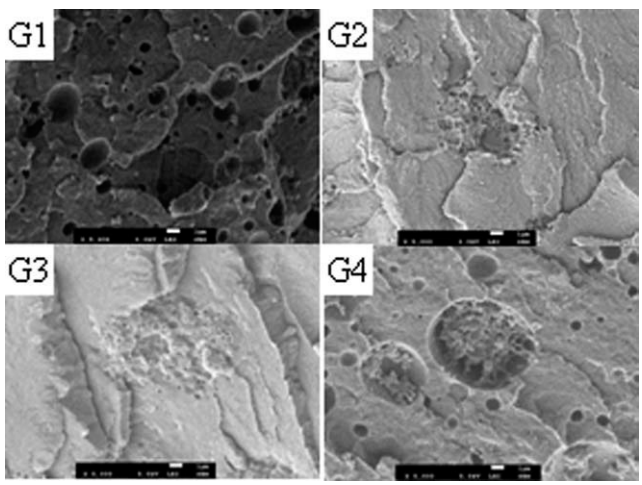

Figure 6 SEM images for the R-PET/ABS (85/15 w/w) blends with various contents of ABS-*g*-MAH (G_1: 0.0 wt %, G_2: 1.0 wt %, G_3: 3.0 wt %, and G_4: 5.0 wt %).

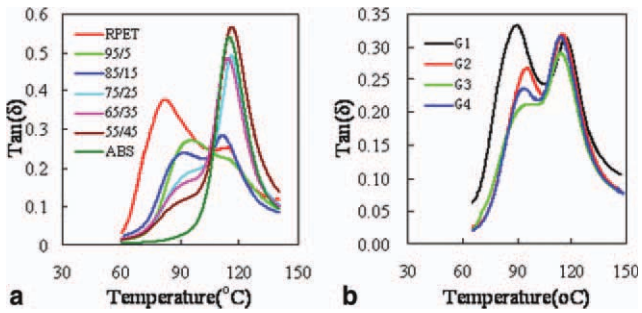

Figure 7 DMA curves for (a) different proportions of R-PET/ABS blends and (b) R-PET/ABS blends with different concentrations of ABS-*g*-MAH (G_1: 0.0 wt %, G_2: 1.0 wt %, G_3: 3.0 wt %, and G_4: 5.0 wt %). [Color figure can be viewed in the online issue, which is available at wileyonlinelibrary.com.]

governed by a number of factors, such as the blend composition, interfacial tension, and viscosity characteristics of the components. The reduction of disperse phase particle dimension with compatibilizer can be attributed to the more effective break-up of the particles, which promote a more stable morphology and ensure improved mechanical properties.[23,24] The above SEM results clearly demonstrate that ABS-*g*-MAH has a compatibilizing effect on the R-PET/ABS blends and that the compatibilization effect becomes more distinct as the ABS-*g*-MAH content increased.

Dynamic mechanical analysis

Dynamic mechanical analysis (DMA) was used to measure the thermodynamic response of R-PET/ABS blends with various blending compositions and R-PET/ABS (85/15 w/w) blends compatibilized by ABS-*g*-MAH with various concentrations and oscillatory deformation in tension–torsion mode as a function of temperature.

The temperature dependences of tan δ for R-PET, pure ABS, and R-PET/ABS blends with various blending compositions are presented in Figure 7(a). In the case of R-PET, two distinct peaks are observed at the temperatures of 82 and 113°C, corresponding to glass transition temperature (T_g) and crystallization temperature (T_c).[25] And, for pure ABS, only one peak is observed at 115°C corresponding to its T_g. For all R-PET/ABS blends, there are two distinct peaks at ~ 90 and 114°C. The first peak corresponds to the T_g of the R-PET matrix ($T_{g\text{-RPET}}$), and the second one relates to the T_g of the pure ABS matrix ($T_{g\text{-ABS}}$). The result suggests that R-PET/ABS blend is a partially miscible system that the two glass transition temperatures are observed and a little approach each other with the blend compositions.[26,27]

TABLE II
Mechanical Properties of R-PET/ABS Blends

R-PET/ABS (w/w)	Notch impact strength (kJ/m^2)	Flexural modulus (MPa)
100/0	1.7	2260
95/5	1.8	1789
85/15	3.9	2374
75/25	3.0	2432
65/35	3.6	2023
55/45	4.9	1973
0/100	13.3	1945

Figure 7(b) shows the temperature dependence of tan δ for R-PET/ABS (85/15 w/w) blends compatibilized by ABS-*g*-MAH with various concentrations of 0.0, 1.0, 3.0, and 5.0 wt % noted as G_1, G_2, G_3, and G_4, respectively. In the tan δ curve corresponding to R-PET/ABS(85/15 w/w) blend with 1.0 wt % ABS-*g*-MAH, the peak for $T_{g\text{-R-PET}}$ shifts from 90 to 95°C, whereas this peak becomes broader but weaker and shifts from 95 to 93 and 92°C, respectively, by raising ABS-*g*-MAH content from 1.0 to 3.0 and 5.0 wt %. The peaks related to $T_{g\text{-ABS}}$ are found to slightly shift to lower temperature region. This result suggests the effective mixing of R-PET and ABS phases in the presence of ABS-*g*-MAH, and this may be due to the common connection of both polymer chains at the interphase, which eventually act as a compatibilizer. The optimum dose of ABS-*g*-MAH is suggested to be 1.0 wt %, and excessive amount of ABS-*g*-MAH leads to little effect on the compatibility of R-PET/ABS (85/15 w/w) system. This is consistent with the results obtained from rheological analysis and SEM microscopy as discussed earlier.

Mechanical properties

Tables II and III show the relationship of mass ratio and compatibilizer concentration with mechanical properties of R-PET/ABS blends. The data of Table I shows that notch impact strength of the R-PET/ABS blends with the presence of ABS is larger than that of R-PET (1.7 kJ/m^2). When ABS content reaches to 15 wt %, notch impact strength raises to 3.9 kJ/m^2, which is two times as that of R-PET. The flexural modulus first increases and reaches to the maximum

TABLE III
Mechanical Properties of R-PET/ABS/ABS-*g*-MAH Blends

R-PET/ABS/ ABS-*g*-MAH (w/w/w)	Notch impact strength (kJ/m^2)	Flexural modulus (Pa)
85/15/0	3.9	2374
85/14/1	5.1	2587
85/12/3	4.9	2496
85/10/5	4.8	2395

value of 2432 MPa at R-PET/ABS mass ratio of 75/25 and attributes to the stress distribution and the crystallinity of PET changed by the presence of ABS. However, it then decreases to 1973 MPa at the mass ratio of 55/45 due to the inferior mechanical properties of ABS to those of R-PET and the transformed of phase structure. The date of Table III shows that the notch impact strength and flexural modulus decrease with the compatibilizer concentration increase, but these values are larger than that of no compatibilizer presence. These are attributed to the compatibilizer increase the interaction of two phase and change the stress distribution.[28,29]

CONCLUSIONS

A series of MA-grafted poly(acrylonitrile-butadiene-styrene) (ABS-*g*-MAH) blends was prepared via melt banbury process on a RM-200B torque rheometer. And the prepared ABS-*g*-MAH polymer was used as a compatibilizer to fabricate recycled poly(-ethylene terephthalate)/poly(acrylonitrile-butadiene-styrene) (R-PET/ABS) blends. The rheology result shows that the grafting action is affected by MA content in ABS and Cole–Cole plots demonstrate that 5 wt % MA is the optimum concentration for preparation of ABS-*g*-MAH. The result of DMA shows that R-PET is partially miscible with ABS, and ABS-*g*-MAH has compatibilizing effects on the R-PET/ABS blends. The presence of ABS-*g*-MAH leads to a shift in glass transition temperatures of R-PET phase in the blend to higher temperatures. The rheological behavior of ABS-*g*-MAH-compatibilized R-PET/ABS blends shows an ABS-*g*-MAH content dependence. However, increasing ABS-*g*-MAH content from 1 to 5 wt % is found to decrease in values of both storage modulus G' and loss modulus G'' of the R-PET/ABS blends, but the values are still larger than that of R-PET/ABS blend without any compatibilizer. The SEM images of the ABS-*g*-MAH-compatibilized R-PET/ABS blends show a finer morphology, confirming the compatibilization effects of the prepared ABS-*g*-MAH.

References

1. Shent, H.; Pugh, R. J.; Forssberg, E. Resour Conserv Recycl 1999, 25, 85.
2. Tao, Y. J.; Mai, K. C. Eur Polym J 2007, 43, 35.
3. Tachwali, Y.; Al-Assaf, Y.; Al-Ali, A. R. Resour Conserv Recycl 2007, 52, 266.
4. Bhattacharya, A.; Misra, B. N. Prog Polym Sci 2004, 29, 767.
5. Li, S. C.; Lu, L. N. J Appl Polym Sci 2008, 108, 3559.
6. Sanchez, S. A.; Calderas, F.; Manero, O. Polymer 2000, 142, 7335.
7. Silva, L. D.; Bretas, R. E. S. Polym Eng Sci 2000, 40, 1414.
8. Fustin, C. A.; Clarkson, G. J.; Leigh, D. A.; Hoof, F. V.; Jonas, A. M.; Bailly, C. Macromolecules 2004, 37, 7884.
9. Kalfoglou, N. K.; Skafidas, D. S.; Kallitsis, J. K. Polymer 1996, 37, 3387.
10. Cook, W. D.; Zhang, T.; Moad, C.; Deipen, G. V.; Cser, F.; Fox, B.; O'shea, M. J Appl Polym Sci 1996, 62, 1699.
11. Cook, W. D.; Moad, G.; Fox, B.; Deipen, G. V.; Zhang, T.; Cser, F.; Mccarthy, L. J Appl Polym Sci 1996, 62, 709.
12. Fakirov, S. Handbook of Thermoplastic Polyesters. Vol. 19; Wiley-VCH Verlag Gmbh: Weinheim, 2002; p 850.
13. Ma, H. Y.; Xu, Z. B.; Tong, L. F.; Gu, A. G.; Fang, Z. P. Polym Degrad Stab 2006, 91, 2951.
14. Chae, D. W.; Byoung, C. K. Compos Sci Technol 2007, 67, 1348.
15. Qi, R. G.; Qian, J. L.; Zhou, C. X. J Appl Polym Sci 2003, 90, 1249.
16. Babbar, I.; Mathur, G. N. Polymer 1994, 35, 2631.
17. Xue, M. L.; Yu, Y. L.; Chuah, H. H.; Rhee, J. M.; Kim, N. H.; Lee, J. H. Eur Polym J 2007, 43, 3826.
18. Madbouly, S. A.; Ougizawa, T. Macromol Chem Phys 2004, 205, 1222.
19. Kim, J.; Kim, J. H.; Shin, T. K.; Choi, H. J.; Jhon, M. S. Eur Polym J 2001, 37, 2131.
20. Aoki, Y. J. Macromolecules 1987, 20, 2208.
21. Carrot, C.; Mbarek, S.; Jaziri, M.; Chalamet, Y.; Raveyre, C.; Prochazka, F. Macromol Mater Eng 2007, 292, 693.
22. Wu, D. F.; Zhang, Y. S.; Zhang, M.; Zhou, W. D. Eur Polym J 2008, 44, 2171.
23. Zhang, H. S.; Guo, W. H.; Yu, Y. B.; Li, B. Y.; Wu, C. F. Eur Polym J 2007, 43, 3662.
24. Hale, W.; Lee1, J. H.; Keskkula, H.; Paul, D. R. Polymer 1999, 40, 3621.
25. Puyvelde, P. V.; Velankar, S.; Moldenaers, P. Curr Opin Colloid 2001, 6, 457.
26. Hale, W.; Keskkula, H.; Paul, D. R. Polymer 1999, 40, 3353.
27. Yoon, K. H.; Lee, H. W.; Park, O. O. J Appl Polym Sci 1998, 70, 389.
28. Gcwabaza, T.; Ray, S. S.; Focke, W. W.; Maity, A. Eur Polym J 2009, 45, 353.
29. Yang, H.; Li, B.; Wang, K.; Sun, T. C.; Wang, X.; Zhang, Q.; Fu, Q.; Dong, X.; Han, C. C. Eur Polym J 2008, 44, 113.